New Nonlinear Design Tools for Self-Oscillating Mixers

Samuel Ver Hoeye, Luis Zurdo, and Almudena Suárez

***Abstract*—New nonlinear design tools for self-oscillating mixers are presented here, with the aim to increase the designer's control over their behavior. The new tools enable fixing the self-oscillation frequency and selecting the optimum self-oscillation amplitude for maximum conversion gain. They can also be applied for the optimized design of harmonic self-oscillating mixers. Using bifurcation-theory concepts, it has been possible to increase the input-power range with self-oscillating-mixer operation. A self-oscillating mixer with 5.5 GHz input frequency has been designed and simulated obtaining very good agreement with the experimental results.**

***Index Terms*—Bifurcation, harmonic mixer, optimization, quasi-periodic regime, self-oscillating mixer.**

I. Introduction

THE self-oscillating mixer (SOM) is a very attractive frequency converter to fulfill requirements of small size, low cost, and low power consumption, since a transistor (or a diode) serves both as a local oscillator and as a mixing element. Due to the self-oscillation, the SOM operates in an autonomous quasiperiodic regime that may be difficult to simulate [1]–[3]. In harmonic balance (HB), special techniques have been provided for SOM analysis [1], [2]. However, the designer often has little control of the SOM self-oscillation frequency, conversion gain and output power and there is a lack of optimization tools.

Here some nonlinear optimization techniques are presented, based on the forcing of the self-oscillation at the desired amplitude and frequency, which increases the designer's control over the SOM performance. The techniques are also suitable for the design of harmonic mixers, with more complex dynamics. Since the SOM-operation bands are delimited by bifurcation phenomena, an additional objective has been the investigation of the possible use of concepts from bifurcation theory to improve the SOM operation. For the sake of clarity, the new techniques are presented through their application to a 5.5 GHz–0.5 GHz downconverter.

II. Nonlinear Optimization of SOM

For the illustration of the technique, a conventional topology is used (Fig. 1). The transistor is an ATF26884. The series feedback at the MESFET source provides negative resistance at the gate port. The IF frequency is selected through a filter at the drain port, also employing an open-circuited $\lambda/4$ parallel line to attenuate the oscillation frequency ω_o.

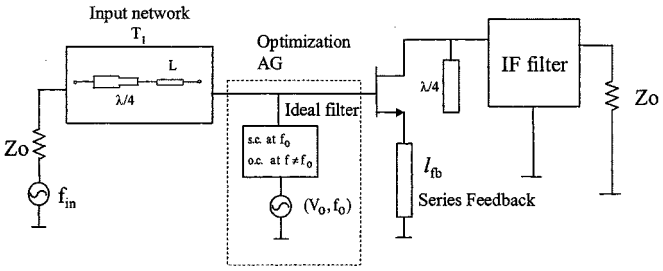

Fig. 1. Conventional SOM configuration, with the inclusion of an AG for optimization purposes.

The design techniques are intended for use in a HB simulator containing optimization routines. They are applied after fulfillment of the oscillation start-up conditions. The techniques are based on the use of an auxiliary generator (AG) [1], [2], only introduced for simulation purposes. A voltage AG is chosen here, connected in parallel at the gate port (Fig. 1). The aim of this generator is to force the self-oscillation at the desired amplitude V_o and frequency ω_o. An ideal filter, in series with the AG, prevents the influence of this generator at frequencies different from ω_o. In order for the generator not to perturb the oscillator steady state, it must fulfill $Y_T = 0$ at its operation frequency ω_o, with Y_T being the AG current to voltage ratio. As will be shown, the AG may be used for different optimization purposes.

A. Free-Running Oscillator

A free-running oscillator is initially designed. The AG frequency $\omega_{\rm AG}$ is made equal to the oscillation frequency that is required for the specified intermediate frequency, $\omega_{\rm AG} \equiv \omega_o = \omega_{\rm in} \pm \omega_{\rm IF}$. Thus, for the 5.5–0.5 GHz downconverter, $\omega_{\rm AG} \equiv \omega_o$ is fixed to exactly 5 GHz. The SOM is expected to provide the highest values of conversion gain for high oscillation amplitude, so, initially, the self-oscillation amplitude has been fixed to $V_{\rm AG} = V_o = 0.8$ V. Here, the preliminary design has been carried out using ideal discrete elements for the input network and the feedback line. The oscillator load (at the gate port), in this preliminary design, is taken as the series connection of a resistance $R_{\rm in}$ and an inductor $L_{\rm in}$. Both elements are optimized to fulfill $Y_T(R_{\rm in}, L_{\rm in}) = 0$. The highest allowed error is $Y_T = 10^{-8} + j10^{-8} (\Omega^{-1})$. In a second design step, the ideal elements are consecutively implemented on microstrip line, using the length l and width w of the corresponding line as optimization variables, with the goal $Y_T(l, w) = 0$. Inclusion of crosses,

Manuscript received May 14, 2001; revised June 19, 2001. This work was supported by the Feder Project 1FD97-0455-C02-01(TIC). The review of this letter was arranged by Associate Editor Dr. Arvind Sharma.

The authors are with the Departamento Ingeniería de Comunicaciones, Universidad de Cantabria, Santander, Spain.

Publisher Item Identifier S 1531-1309(01)07974-0.

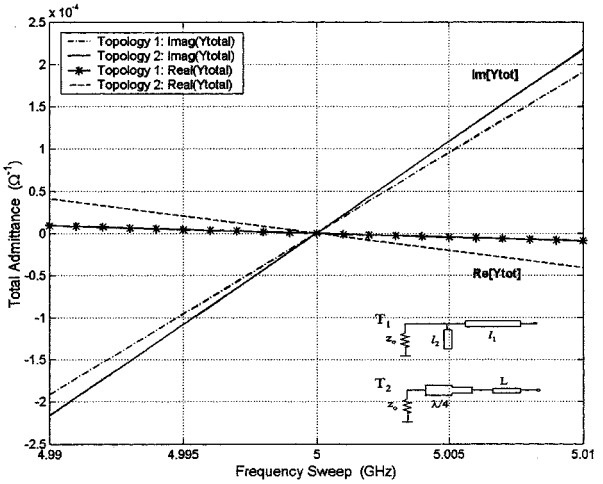

Fig. 2. Evaluation and improvement of the frequency selectivity of the free-running oscillator. Two different topologies for the oscillator load (*input network*, at the gate port in Fig. 1) are compared.

tees, or steps also requires slight line optimization. Two different topologies, for the implementation of the oscillator load, are compared in Fig. 2. The one with higher frequency selectivity (T_2) has been chosen. Due to the potential instability of the oscillator, the stability of the final design must be checked.

B. Self-Oscillating Mixer

For self-oscillating mixer operation, the input generator is connected. Here, constant input power $P_{\rm in} = -16$ dBm and frequency $f_{\rm in} = 5.5$ GHz have been considered. Re-optimization of linear elements is necessary to maintain the same self-oscillation frequency $f_o = 5$ GHz and amplitude $V_o = 0.8$ V. The same condition $Y_T = 0$ is imposed, now using multitone HB. For the particular generator value, it is also possible to sweep V_o (forced through the AG), at constant self-oscillation frequency (and thus constant $\omega_{\rm IF}$) to select the most suitable V_o value in terms of SOM conversion gain [Fig. 3(a)]. Here, the input network has been kept fixed for this analysis, optimizing, for each V_o, the length of the feedback line (l_{fb}) and the $V_{\rm GS}$ bias (with constant $V_{\rm DS} = 3$ V). A smooth curve is obtained (Fig. 3) that provides the conversion gain versus V_o. Beyond $V_o = 1.1$ V, optimization was not possible. The performance of different designs, with exactly the same $\omega_{\rm IF}$, can thus be compared. The selected values were $l_{fb} = 7.3$ mm and $V_{\rm GS} = -0.27$ V (experimental point). Optimization of the $V_{\rm GS}$ and $V_{\rm DS}$ bias provides essentially the same curve [Fig. 3(a)]. The results in terms of these voltages (of more general interest) are traced versus V_o in Fig. 3(b).

The same technique can be used for the design of harmonic SOM. In these circuits, the input frequency mixes with a given harmonic $n\omega_o$ of the self-oscillation frequency, to provide $\omega_{\rm IF} = \omega_{\rm in} \pm n\omega_o$. The quality factor is not usually very high, to enable the harmonic generation. The new technique enables fixing the oscillation fundamental frequency at ω_o. Just as an illustration, the conversion gain of the former SOM as second-harmonic mixer (with $f_{\rm in} = 10.5$ GHz) has been evaluated in Fig. 3(c), also tracing the conversion gain versus

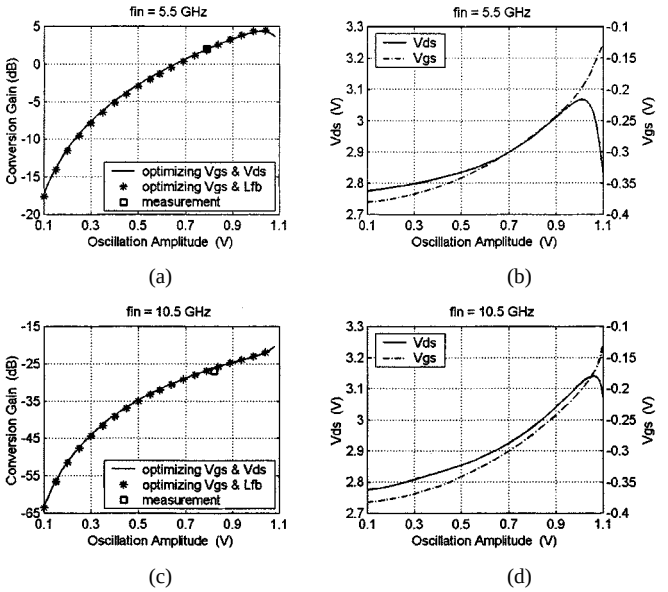

Fig. 3. (a) Conversion gain versus self-oscillation amplitude V_o for $f_{\rm in} = 5.5$ GHz and constant IF frequency $f_{\rm IF} = 0.5$ GHz. (b) Transistor bias voltages for each V_o value in (a). (c) Conversion gain versus self-oscillation amplitude V_o for $f_{\rm in} = 10.5$ GHz and constant IF frequency $f_{\rm IF} = 0.5$ GHz. (d) Transistor bias voltages for each V_o value in (c). The experimental points correspond to actual designs.

the oscillation amplitude. The bias voltages corresponding to each V_o are shown in Fig. 3(d).

III. Increasing the SOM Operating Ranges

When varying the input generator power $P_{\rm in}$ or frequency $\omega_{\rm in}$, two different phenomena delimit the mixing-operation ranges [Fig. 4(a)]: the synchronization between the two fundamentals ($\omega_{\rm in}$ and ω_o) and the inverse Hopf bifurcation [1]. In the plane $P_{\rm in}$–$\omega_{\rm in}$, the synchronization locus is typically located in the lower input-power range [Fig. 4(a)] and centered about ω_o. Here, it is obtained for input power below $P_{\rm in} = -25$ dBm. The inverse Hopf bifurcation, or asynchronous extinction of the self-oscillation, leads to a periodic regime, with $f_{\rm in}$ as only fundamental.

The increase in the SOM input-power range can be achieved by increasing the input-power value at which the inverse-Hopf bifurcation takes place, $P_{\rm in} = P_{inH}$. As this bifurcation is approached, the oscillation amplitude continuously decreases to zero, usually with high slope. Thus, P_{inH} can be practically imposed by setting the AG to a negligible amplitude $V_o = \varepsilon$ (for this input-power value). Note that the actual Hopf bifurcation takes place for $V_o = 0$. The increase in the input-power range is better achieved in several consecutive optimizations, gradually increasing P_{inH}. Here, a couple of variables (lengths and widths in the load and feedback circuits) have been modified in each optimization step, with $V_o = \varepsilon = 10^{-2}$ V and $f_o = 5$ GHz. Imposing this value for the self-oscillation frequency at the inverse Hopf bifurcation might lead to a shift of the self-oscillation frequency in the low input-power range, due to the autonomous nature of the circuit. A compromise can be obtained by re-optimizing the circuit in the absence of the generator, at

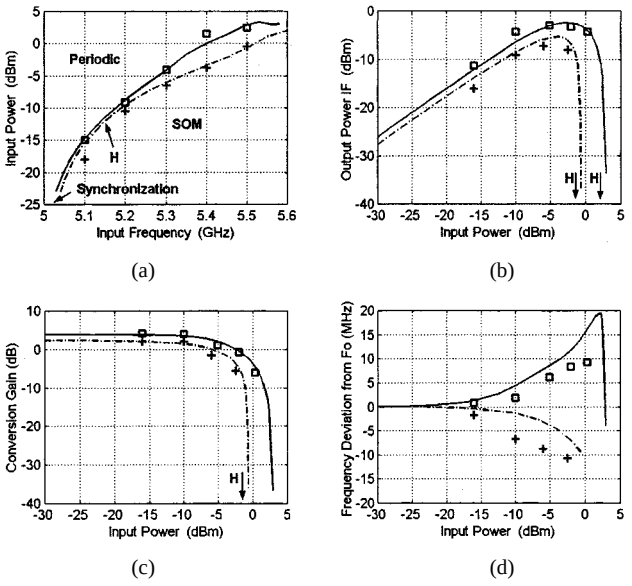

Fig. 4. Increase of the SOM input-power range. Dashed line: Design of Section II-B. Solid line: new design (Section III). (a) Hopf-bifurcation locus. The SOM operation region is located, for each design, below the corresponding curve. (b) Output power at IF frequency. (c) Conversion gain. (d) Deviation of the self-oscillation frequency from the desired value 5 GHz.

each step, using different variables. The two consecutive optimizations, for each P_{inH} step, $P_{inH} = P_{inH}^{k}$, (up to the maximum achievable value) are outlined in the following

$$Y_T(\gamma_1, \gamma_2) = 0 \quad \text{with } V_o = 10^{-2}\ \text{V},\ f_o = 5\ \text{GHz},\ P_{\text{in}} = P_{inH}^{k}$$
(Inverse Hopf)

$$Y_T(\gamma_1', \gamma_2') = 0 \quad \text{with } V_o = 0.8\ \text{V},\ f_o = 5\ \text{GHz},\ P_{\text{in}} = 0\ \text{W}$$
(Free-running oscillator).

With (γ_1, γ_2) and (γ_1', γ_2') being two different sets of optimization variables. In this particular circuit, variables in the input network were optimized to increase P_{inH}, while the feedback line (in length and width) was optimized for fixing the free-running frequency.

The results of the optimization are shown in Fig. 4(a)–(d) and are compared with the design in Section II-B. As can be seen, it has been possible to increase the SOM maximum input power from $P_{inH} = -1$ dBm to $P_{inH} = 3.5$ dBm [Fig. 4(a)]. Fig. 4(b)–(d) were obtained for constant input frequency $f_{\text{in}} = 5.5$ GHz, varying P_{in}. The extinction of the solution paths is due to the extinction of the self-oscillation (inverse-Hopf bifurcation). Fig. 4(b) shows the evolution of the IF output power and Fig. 4(c), the conversion gain. The 1 dB gain-compression point has been increased from $P_{\text{in}} = -4.54$ dBm to $P_{\text{in}} = -1.65$ dBm. Fig. 4(d) shows the evolution of the self-oscillation frequency. Both the old and new designs have the value $f_o = 5$ GHz in the low P_{in} range. Limited variations of this frequency are also obtained in the whole P_{in} range [Fig. 4(d)]. Note that these variations could be reduced using a technology with higher quality factor [4]. If the Hopf-bifurcation locus is smooth enough, the optimization will affect, as in this case [Fig. 4(a)], the neighboring frequencies, with an overall extension of the SOM operation region.

IV. Conclusions

Some tools have been provided for an optimum design of self-oscillating mixers. The tools allow fixing the self-oscillation frequency, for accurate frequency conversion, and the self-oscillation amplitude, for maximizing the conversion gain. Use is also made of bifurcation-theory concepts to increase the input-power range with self-oscillating mixer operation. A 5–0.5 GHz downconverter has been designed with these techniques, obtaining excellent experimental results.

References

[1] J. Morales, A. Suárez, E. Artal, and R. Quéré, "Global stability analysis of self-oscillating mixers," in *25th Eur. Microw. Conf.* , Bologna, Sept. 1995, pp. 1216–1219.

[2] A. Suárez, "Self-oscillating mixer circuits. Stability analysis," in *IEEE MTT-S Dig.*, Jun. 2000.

[3] M. Claassen and U. Güttich, "Conversion matrix and gain of self-oscillating mixers," *IEEE Trans. Microwave Theory Tech.*, vol. 39, pp. 25–30, Jan. 1991.

[4] G. C. Wang, T. J. Lin, W. C. Liu, and S. Y. Yang, "A low cost DBS low noise block downconverter with a DR stabilized MESFET self-oscillating mixer," in *IEEE MTT-S Dig.*, 1994, pp. 1447–1450.